2024 IEEE International Conference on Robotics and Automation (ICRA 2024)
May 13-17, 2024. Yokohama, Japan

Everyday finger: a robotic finger that meets the needs of everyday interactive manipulation

Rubén Castro Ornelas, Tomás Cantú, Isabel Sperandio, Alexander H. Slocum, and Pulkit Agrawal
Improbable AI Lab Massachusetts Institute of Technology

***Abstract*— We provide the mechanical and dynamical requirements for a robotic finger capable of performing a large number of everyday tasks. To match these requirements, we present a novel actuator and finger design, the everyday finger, that comes close to many characteristics of the human fingers. In particular, we focus on minimizing the size of components to get proper performance without sacrificing compactness. A robotic hand that uses two Everyday fingers demonstrated an 80% success rate in picking up and placing dishes in a rack, and the ability to pick up flat objects like napkins and delicate ones like strawberries. Videos are available at the project website: `https://sites.google.com/view/everydayfinger`.**

I. INTRODUCTION

Enabling robots to manipulate human tools has been a long-standing challenge and dream in robotics. When attempting fine, dexterous, and forceful manipulation in human environments designed around human bodies, incorporating some properties of human hands, like their size, morphology, and compliance, into a robotic manipulator can be advantageous. Building human-like multi-finger hands is well researched [5, 21], but a satisfactory manipulator for dexterous manipulation doesn't exist. The primary challenges have been: (i) The difficulty of controlling large degrees of freedom system for contact-rich manipulation. However, recently, reinforcement learning has emerged as a promising method for controlling dexterous hands [3, 9, 13, 18, 30]. (ii) Properly balancing the tradeoff between the manipulator's size, compliance, durability, and the power it can provide. As an example, for the fingers to exert a large force, high torque is necessary but such actuators usually have a big form factor making the fingers bulky and thereby making the hand incapable of using many human tools purely from a geometric standpoint.

To achieve the requisite torque and velocity objectives within a compact hand, many dexterous robotic hand designs such as the Robonaut II [7], Shadow hand [23], or DLR hand [12] and others [6, 16, 22] house motors in a forearm and route tendons to the fingers. While this design sidesteps the challenge of miniaturizing the actuator, it adds complexity through intricate transmission systems, a cumbersome forearm, and a high manufacturing cost. Additionally, tendons must pass through a moving wrist. All these parts decrease reliability. Shadow dexterous hand, one of the most popular robotic hands, is known to be a challenge to work with due to breakages and maintenance being complicated [20] due to the complex design. For these reasons, we avoided the use of a tendon-driven mechanism.

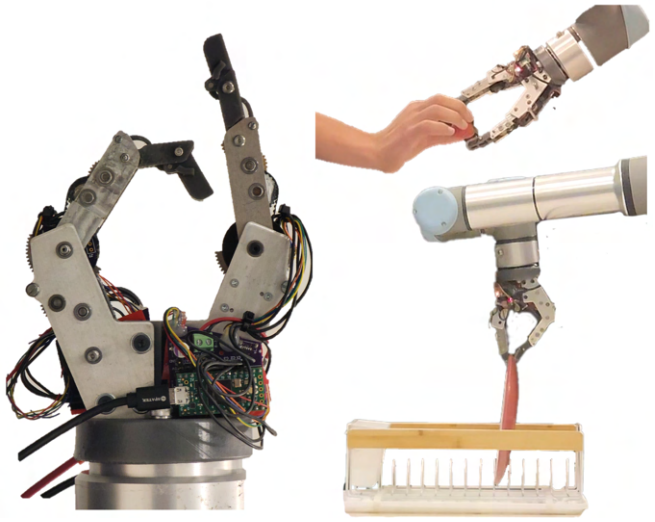

Fig. 1: The proposed design of the *everyday* two-finger robotic hand that is appropriate for daily tasks.

A range of recent robotic hands, like the Allegro hand [1] and the Leap Hand [24], use off-the-shelf actuators to directly drive joints, emphasizing minimal custom parts to keep costs low and increase the accessibility of robotic hands. While these models serve research objectives effectively, their reliance on off-the-shelf components often results in a bulkier build (1.5-3x times the human hand), which complicates their utility for manipulating tools designed for human use.

The key missing piece to having a robotic hand that is similarly sized to a human hand is therefore a good actuator design. Qualitatively, for a robotic hand to be useful for everyday tasks, we need it to be forceful, speedy, high bandwidth, compliant, and compact. A useful robotic hand can exert enough **force** so that it can firmly hold heavy objects like a milk jug and use tools. At the same time, it needs to have enough **speed** and **bandwidth** in order for the hand to be used for dynamic tasks such as re-orientation. While one might assume it's acceptable for robotic hands to move slower than humans, finger speed serves a broader purpose. If an object slips and begins to fall during re-orientation, the fingers must swiftly adjust to catch it. Hence, quick finger movements are not just about efficiency, but also ensuring task reliability and a higher success rate in handling disturbances. **Compactness** allows the robotic hand to use human tools. If the hand is too big, it will struggle to pick up smaller and flat objects and is impossible for it to

979-8-3503-8457-4/24/$31.00 ©2024 IEEE

operate certain tools such as scissors. Lastly, a useful robotic hand also has **compliance**, which enables contact-rich tasks and makes high-level planning easier. Consider reaching for a wooden block on a table: even with misalignment, compliant fingers can adapt to the table's surface, allowing it to guide the fingers to the block. This not only improves grasp reliability but also protects against potential damage from unforeseen impacts, facilitating safer and more versatile interactions with various objects and surfaces in dynamic environments.

Despite a large body of work on hand design, to the best of our knowledge, there is no quantitative characterization of the *five key traits of compactness, compliance, force, speed, and bandwidth* of actuators for performing everyday tasks. Our first contribution is to provide quantitative values of these critical metrics/traits of robotic hands that would enable them to perform everyday tasks (Section III). Based on this analysis, we show that it is now possible to design an actuator that satisfies all the requirements. The reason we are able to do so is: (i) our design choice prioritizing common daily tasks over extreme human performance capabilities (ii) the increased availability and miniaturization of torque-dense electric motors. We propose a new actuator design that satisfies the specifications required for everyday tasks. Using this actuator, we built a two-finger robot hand to empirically verify its performance on key functional requirements and demonstrate its potential in performing everyday tasks (see Fig 1).

II. Other Prior Works

A. Soft hands

Soft robotic hands offer delicate handling that rigid hands might struggle with [25]. Their inherent compliance can make them adept at tasks like handling fruit. However, accurately simulating the complex dynamics of soft materials presents a significant challenge. Traditional simulation environments may not accurately capture the nuanced behaviors of soft robots. Because of this, using the latest reinforcement learning control and Sim2Real techniques may not be possible for soft robots until simulators become faster. This constrains the immediate applications for soft robotic hands. We need to find a way to add compliance while not limiting the simulatability of the hand.

B. Similarities between manipulation and locomotion

Robotic quadrupeds is another field that has benefited from the advancements in brushless motor technology and from introducing compliance. Proprioceptive actuators, like in the MIT Cheetah [28], have enabled fast, contact-rich, and dynamic movements from robot quadrupeds. Series Elastic Actuators (SEAs) like those in the ANYmal robot dog [15] have also enabled stable contact interactions with the environment, albeit with lower bandwidth. We can gather many insights by looking at the design techniques for robot quadrupeds. They use low-inertia actuators with high torque density, high transmission transparency, and capability for simulation. In particular, one prevailing debate in this field centers around the necessity of SEAs. We employ a similar analytical framework used for the MIT Mini Cheetah [17] in Section IV to design our actuator.

III. Functional Requirements

Our first goal is to characterize the strength, speed, bandwidth, and compliance requirements for a robotic hand that is as compact as a human hand and can still apply forces large enough to perform everyday tasks. We will now detail how we obtained such a characterization. The results are summarized in Table I.

A. Force, Bandwidth, and Speed Characterization

It is important for a finger to not only apply forces, and move fast, but also be able to quickly transition between different forces (i.e., bandwidth). To obtain these quantities for everyday tasks, we used a prior study that reported force/torque measurements of humans performing 30 different daily tasks [14]. We mapped these measurements to torques experienced at each joint of a model hand with three fingers, with 3 DOFs each. The three joints per finger can be seen in Figure 2, and are the Proximal Interphalangeal (PIP), Metacarpophalangeal Z-axis (MCP-Z), and the Metacarpophalangeal X-axis (MCP-X).

Obtaining torques at the joints based on FT sensor readings of tools is an under defined problem with many solutions, so it is impossible to outline a closed form solution. Because of this, we use an optimization algorithm that minimizes the sum of the fourth powers of the joint torques to penalize high peak torques. To set up our optimization, we made a few assumptions. The most critical assumptions are: (Assumption 1) The fingers statically grip a cylindrical handle for each task. We used cylinders with three different radii: 8mm (small), 15mm(medium), and 22mm(large). For each task, we chose a size that resembles our estimate of the real-world handle size of each task (see Fig. 2). For a stronger grip, some tasks (i.e. using hammer to hammer in nail) also incorporate a 4th touch-point on the cylinder (a "palm"). The configuration of handle radius, presence of palm, and exact grasp points for each task is given in the Appendix on our website. As different tasks usually require heavily customized different grips/handles and we're bucketing them, this method does not give the optimal lowest torques the finger can ever experience but rather gives a reasonable upper bound. This gives us six equations for force and moment balance (Eqns. 2-7), and friction cone constraints on each touch-point (Eq. 8). (Assumption 2) We also assume that the fingertip force will lie somewhere in a 8mm radius circle of the center of the fingertip. This makes sense as a "center of pressure" since the contact is not a single point. The palm force point, if present, has a 20mm radius available (Eq. 9). (Assumption 3) Coefficient of friction of 0.6. In the real world, this varies wildly depending on skin moisture, materials being handled, age, and more. For our purposes, we chose 0.6 to be a reasonable average scenario. For reference, dry skin on glass has coefficient of friction of 2.18 ± 1.09 [10]. (Assumption 4) The force due to gravity of the tools is

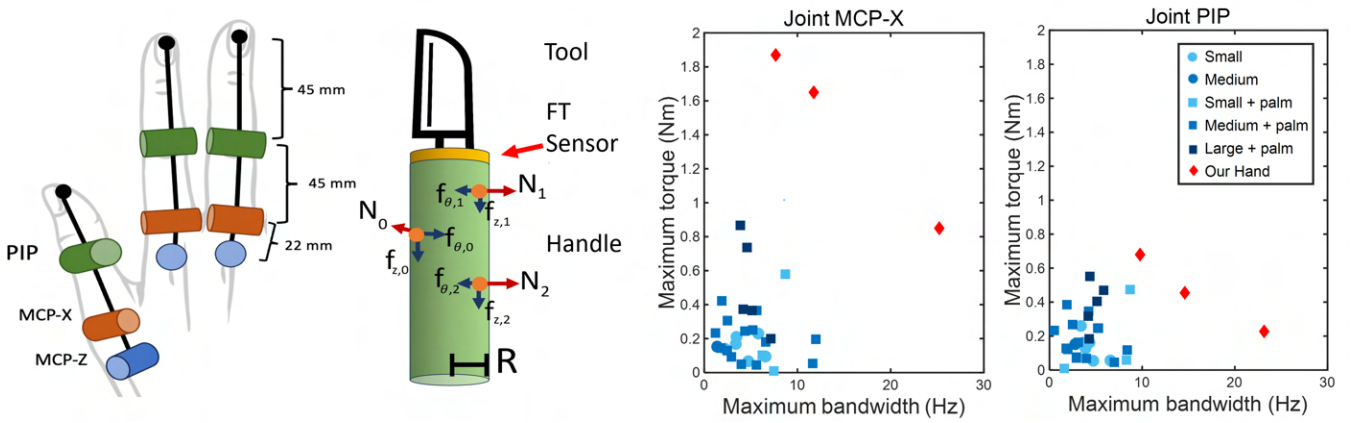

Fig. 2: Left: Finger geometry and degrees of freedom used in optimization. Left-Middle: diagram of three contact points (orange) on a cylindrical tool handle and their corresponding forces as used in optimization. Right: Our hand's capabilities compared to daily task requirements. Tasks are split between small, medium and large handle radius, as well as whether 4th contact paint, a palm, was used.

measured by the FT sensor used in the force studies, but we ignore gravity effects of the fingers. The weight of the finger contributes less than 5% to the maximum output torque of each motor in the worst case. We also note that MCP-X and MCP-Z are usually co-located at the same point. However, to avoid using ball joints, we separate them slightly and put them in series.

From the obtained torque trajectories, we computed the maximum torque and bandwidth required to follow the planned trajectory closely on each of the three joint types in the analysis (PIP, MCP-Z, MCP-X) for the 30 different daily tasks. To find the bandwidth required, we simulate first order systems with a range of bandwidths and find the minimum bandwidth in which the output has 98% of the time steps within 5% of the reference torque trajectory signal. We note that this method is not perfect since the tool demonstrations do not represent a minimum amount of effort to complete the task, but rather the default of the person doing the demo. This still serves to establish a reasonable estimate of the torques and bandwidth we expect from our robotic finger design.

The optimization problem is described next, Where F and T are the measured forces and torques from the FT sensor in each direction, N_i are the touch-point forces normal to the cylinder, the f are the friction forces in θ and z components of the cylinder frame, R is the radius of the cylinder, $\mu = 0.6$ is the assumed coefficient of friction. z_i, θ_i are the locations of the actual touch-point forces at each time step around the cylinder, and $\bar{z}_i$, $\bar{\theta}_i$ are the locations of the center of the touch-point pressure areas (Subscript 3 refers to the palm, when available), and $r_{presssure}$ is the radius of the touch-point pressure area. For each finger (i=0,1,2), $\tau_{MCPZ,i}, \tau_{MCPX,i}, \tau_{PIP,i}$ are the torques on each joint. J is the jacobian matrix between the fingertip forces and the joint torques. This matrix depends on the length, position, and orientation of the joints with respect to the cylinder.

The results from each task in the database are in Figure 2.

$$\min \quad \sum_{i=0,1,2} \tau^4_{MCP-Z,i} + \tau^4_{MCP-X,i} + \tau^4_{PIP,i} \tag{1}$$

$$\text{s.t.} \quad F_x = \sum_{i=0,1,2,3} (N_i \cos\theta_i - f_{\theta,i} \sin\theta_i) \tag{2}$$

$$F_y = \sum_{i=0,1,2,3} (N_i \sin\theta_i + f_{\theta,i} \cos\theta_i) \tag{3}$$

$$F_z = f_{z,0} + f_{z,1} + f_{z,2} + f_{z,3} \tag{4}$$

$$T_x = \sum_{i=0,1,2,3} (-z_i(N_i \sin(\theta_i) + f_{\theta,i} \cos\theta_i) + R \sin\theta_i f_{z,i}) \tag{5}$$

$$T_y = \sum_{i=0,1,2,3} (z_i(N_i \cos\theta_i - f_{\theta,i} \sin\theta_i) - R \cos\theta_i f_{z,i}) \tag{6}$$

$$T_z = R(f_{\theta,0} + f_{\theta,1} + f_{\theta,2} + f_{\theta,3}) \tag{7}$$

$$f^2_{\theta,i} + f^2_{z,i} \leq (\mu N_i)^2 \qquad \text{for } i = 0,1,2,3 \tag{8}$$

$$(z_i - \bar{z}_i)^2 + R^2(\theta_i - \bar{\theta}_i)^2 \leq r^2_{pressure} \qquad \text{for } i = 0,1,2,3 \tag{9}$$

$$\begin{bmatrix} N_i \\ f_{z,i} \\ f_{\theta_i} \end{bmatrix} = J \begin{bmatrix} \tau_{MCP-Z,i} \\ \tau_{MCP-X,i} \\ \tau_{PIP,i} \end{bmatrix} \text{ for } i = 0,1,2 \tag{10}$$

Speed: To obtain a measure of the maximum speed that a human finger can operate at, we obtained the data from a prior work analyzing the maximum speed of an expert pianist's finger while playing piano. [8]. While this is an overestimate as to what is required to do daily tasks, we could not find experimental data to base a value off of, and would be an interesting project for further research.

B. Compactness

To ensure compatibility with human tools, our design's size constraints are grounded in a study that examined the bone and soft tissue measurements of human fingers [27].

TABLE I: Comparison of Desired and Achieved Functional Requirements

Functional Requirement	Desired	Ours	Pass
PIP Torque (Nm)	0.55	0.68±0.01	✓
PIP Bandwidth(Hz)@0.55Nm	8.69	14.6±2.53	✓
PIP Torque to backdrive (Nm)	0.11	0.022±0.005	✓
PIP Maximum Speed (rad/s)	4.5	21.6±0.2	✓
MCP-X Peak Torque (Nm)	0.86	1.87±0.07	✓
MCP-X Bandwidth(Hz)@0.86Nm	11.96	25.2±0.1	✓
MCP Torque to backdrive (Nm)	0.11	0.094±0.006	✓
MCP Maximum Speed (rad/s)	4.5	9.8±0.3	✓
Width (Finger) (mm)	22.4	15	✓
Width (Knuckle) (mm)	22.4	36	✗
Height (Finger) (mm)	22.4	9	✓
Height (Knuckle) (mm)	22.4	28	✗
Length of Finger (mm)	104.2	90.5	✓

The maximum expected length of a human index finger, calculated as the mean length plus three standard deviations, is 104.2 mm for bone and an additional 5.61 mm accounting for soft tissue. For finger width, we followed the dimensions provided in [27], which align closely with typical human hand widths, giving us a width allowance of 22.4 mm per finger, including soft tissue. We use the same value of 22.4mm for the height of the finger for symmetry. Note that we choose to focus on geometry of the actual fingers and not so much on the palm. The palm is subject to further study, however, there is more geometric leniency when designing a palm (i.e. the back of the hand can be thicker without loss in ability).

C. Compliance

The compliance requirement defines how much force an object being interacted with must exert on the robot fingers to push them back. Ideally, this force to push back the robot is light enough that delicate objects such as fruit can push back the fingers without damaging the fruit, or such that a finger hitting a table doesn't damage it and instead can be used as a guide. In order to handle these scenarios, we wanted the maximum torque to backdrive the finger from static to be 0.11Nm for the each joint. This means it can be back driven with 1 N at the fingertip, which is light enough to not damage most surfaces.

IV. Proposed Finger Design

We now describe an actuator and finger design that closely matches desired functional characteristics derived in the previous section. The actuator is tested using a proof-of-concept two-finger robotic hand with 4 DOF (two DOFs per finger). There are three main components in our design: the motor, the transmission stiffness/elastic element, and the PIP to DIP 4-bar linkage. The motor defines how much power we can get. The stiffness determines how much torque our system will experience with a given impact and also defines the bandwidth of the finger. The 4-bar linkage allows us more delicate control of objects just touching the fingertips.

A. Motor

The torque generated by a motor, τ_{motor}, can be approximately derived using the maximum electromagnetic shear stress, τ_{em}, across the area of the stators with Diameter D and length L of the motor and the gear ratio, N. The value of τ_{em} can be obtained from engineering tables [26].

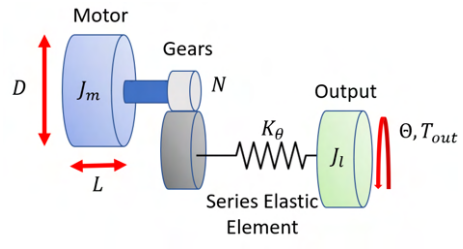

Fig. 3: Classic model for a series elastic actuator.

$$\tau_{motor} = N\tau_{em}\frac{D}{2}(\pi DL) \tag{11}$$

Due to the increase in demand for brushless motors, the maximum torque density available from commercial motors has increased. We were able to find a motor (28mm OD x 14mm L) for the PIP joint which is slightly larger from the size specified by using the above equation with our functional requirements. For the MCP joint, we could not find a motor that was close to the theoretical recommended size, so we use a motor that is oversized (34.5mm OD x 15.7mm L). That's why we exceed our functional requirements for our MCP joint by quite a margin. Keeping the reflected inertia low allows our bandwidth to be higher [4], so we chose maintain a small gear ratio (≤ 15). More details on the motors chosen can be found in the Appendix on our website.

B. Transmission Stiffness

The stiffness of our transmission determines the bandwidth and the peak torque experienced during impact. The transmission can be made very stiff which would increase the bandwidth, but also result in higher peak torques during impact necessitating stronger transmission. On the other hand, to make the finger resistant to impact, the transmission can be made very elastic (i.e., less stiff), but then it will result in low bandwidth which is insufficient for agile behaviors. Our desire is to achieve the maximum possible bandwidth while limiting peak impact torque to be lower than the strength of our transmission which corresponds to the torques at which the gears break. The peak impact torque can be calculated by analyzing a full-speed collision of the finger against an immovable object [17]. In this case, all the inertial energy from the motor ($\frac{1}{2}J_m N^2 \dot{\theta}^2_{max}$) will be absorbed by transmission with stiffness k_θ which lead to an angular deflection in the finger by the amount $\Delta\theta_{max}$. Here J_m is motor inertia, N is the gear ratio, $\dot{\theta}_{\max}$ is the maximum speed of the motor. The maximum motor displacement can therefore be calculated as:

$$U_{spring} = \frac{1}{2}k_\theta \Delta\theta^2_{max} = \frac{1}{2}(J_m)\, N^2 \dot{\theta}^2_{max} \tag{12}$$

$$\Rightarrow \Delta\theta_{max} = N\dot{\theta}_{max}\sqrt{\frac{J_m}{k_\theta}} \tag{13}$$

The peak torque from the collision, $\tau_{collision}$ will be experienced at this maximum spring displacement and can be calculated as following:

$$\tau_{collision} = k_\theta \Delta\theta_{max} = N\dot{\theta}_{max}\sqrt{k_\theta J_m} \tag{14}$$

From here, we can equate the maximum torque experienced to the strength of the transmission, $\tau_{collision} = \tau_{strength}$, in our case the torque at which the gears break, and we can find what our maximum k_θ can be.

$$k_\theta^{\max} = \frac{\tau_{strength}^2}{(N\dot{\theta}_{max})^2 J_m} \tag{15}$$

Now that we have the maximum stiffness, we need to find the minimum stiffness based on the desired bandwidth specification and the system's inertia. For this computation, we make a first order approximation of the bandwidth B to the natural frequency ω_n of the transmission. The natural frequency of the transmission can be derived as follows:

$$B \approx \omega_n = \sqrt{\frac{k_\theta^{min}}{J_m N^2}} \tag{16}$$

$$k_\theta^{\min} = \omega_n^2 J_m N^2 \tag{17}$$

Using the values of $\omega_n, J_m, N, \tau_{strength}, \dot{\theta}_{max}$ from our parts and specifications, we obtain a range of possible values for the stiffness between: k_θ^{min} = 2.24 Nm/rad and k_θ^{max} = 10.16 Nm/rad. This range is low enough that it requires a spring in series in order to reach this regime of stiffness. While there has been success with propioceptive actuators without a spring in series for quadrupeds, for robotic hands, it looks like a spring is required to sustain impacts and reach the low stiffness levels required.

C. Design of the Elastic Element

The main challenge in inserting a spring in the transmission is packaging so that we still can satisfy the size requirements. We solve this by customizing one of gears in the transmission to have compliance internally. More details are provided in the Appendix on our website.

D. 4-bar linkage

With inspiration from Psyonic Ability hand [2], in order to get the same action as the human finger's DIP joint, we added a 4-bar linkage between the DIP joint and the PIP joint of the robotic hand, as illustrated in Figure 4. This design choice effectively constrains the PIP joint actuator's output to the DIP joint, ensuring the robotic finger emulates the characteristic curling motion observed in human fingers. Moreover, we intentionally designed this linkage with an 'S' shape, allowing it to also act as a spring. This added feature imparts additional compliance to the fingertip, making it better at handling delicate tasks that just engage the fingertip such as handling small objects.

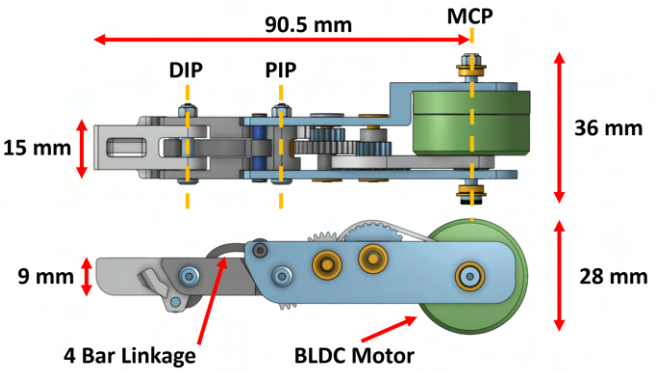

Fig. 4: Everyday robotic finger measurements and design, without MCP actuator.

V. Experiments and Discussion

There are two primary goals of our experiments: first, to characterize the performance of our actuator/finger along the five key design traits. The second goal is to qualitatively evaluate the performance of the robotic fingers on a few representative tasks that require compact size, force application, speed, and compliance. We chose these tasks as picking and placing dishes in a dish rack, pickup of strawberries, and picking a napkin lying flat on a table.

A. Characterization experiments

For the characterization experiments we mounted one finger on a Universal Robot's UR5 arm. It's important to note that there are two actuators within each finger: the MCP-X and the PIP joint actuator.

1) Torque and bandwidth characterization: In order to evaluate the maximum torque we can exert, we placed a Vernier Dual-Range Force sensor 45 mm away from the MCP-X joint, underneath the PIP joint. By measuring the maximum force that the finger exerts at this point, we can calculate the maximum torque that can be produced by the MCP-X joint. Simultaneously, we measure the rise time of our torque output, calculated as the time it takes to go from 10% to 90% of the desired torque, which can be used to estimate the torque bandwidth of the system at a given torque. Given the rise time, t_r, the bandwidth is in the literature commonly approximated as [19]: $B(Hz) = 0.35/t_r(s)$. We used the same method for the PIP joint.

Based on our data, the MCP joint has a peak torque of 1.87Nm, and the PIP Joint of 0.68Nm. The bandwidth changes for each commanded torque, and various datapoints can be seen on Figure 2, which clearly show we can meet the bandwidth requirements of our sample tasks.

The MCP joint outputs about 2x more torque than required. Ideally in the future, we can have more options for brushless motors of this size category which would allow us to pick a smaller motor which gives us just the performance we need.

2) Compliance: To measure compliance, we used the same setup as the torque experiment and had the UR5

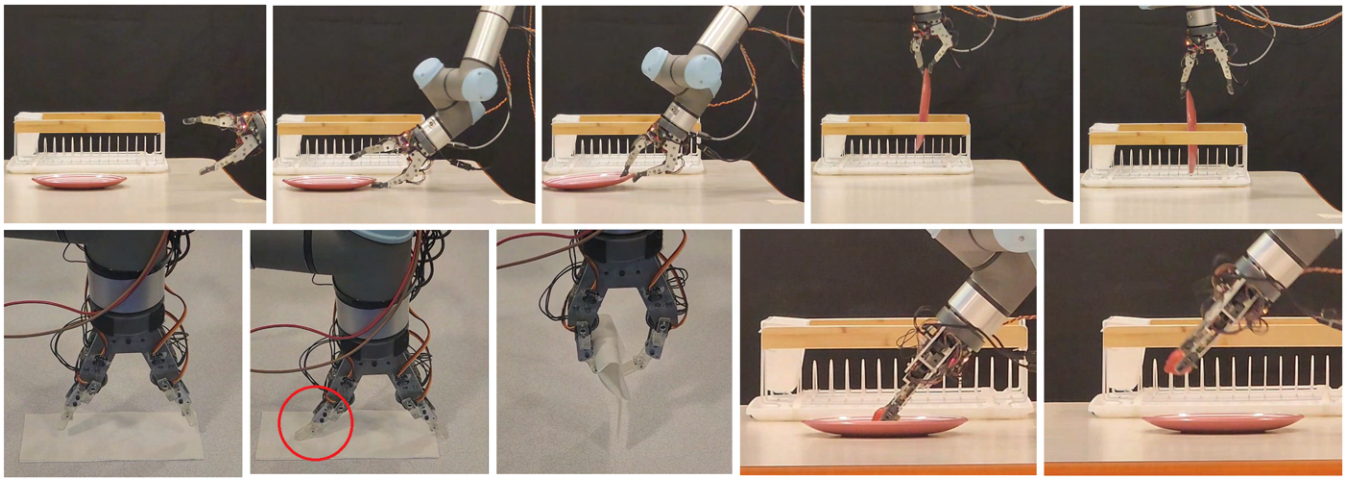

Fig. 5: Qualitative tests run with the Everyday two-finger hand: (1) picking up and placing a dish. (2) picking up a flat napkin, and (3) picking up a strawberry without damaging it.

lower the finger into the force sensor at the maximum allowed manual control speed, starting from 5cm above the sensor, with the motor off until the finger moved about 45 degrees. After five trials, we measured the torque to push back the finger at 0.094±0.006 Nm for the MCP joint, and 0.022±0.005 Nm for the PIP joint.

3) Speed: The maximum speed of the PIP and MCP joints was measured by moving the finger from one end of its limit to the other. The finger position is measured using the internal magnetic encoders. We found the maximum and stable speed to be 9.8±0.3 rad/s for the MCP Joint and 21.6±0.2 rad/s for the PIP Joint.

4) Compactness: Our finger was more compact than the functional requirements for most of the finger. However, due to the size of the motor, the knuckle was larger than the desired width.

B. Qualitative Experiments

For the qualitative experiments, we mounted the full two-finger robotic hand that uses the Everyday finger to a Universal Robots UR5 robotic arm, and hardcoded a fixed trajectory for each task.

1) Fast dish Pick and place: This task highlights the main unique points of this hand: it's compactness and compliance. While many robotic hands rely on a complex planned out routine to pick up dishes by pushing them against a wall [29] [11] or towards the edge of the table, our fingers can simply hit the table, comply against the table, and then slide underneath the dish lip to grasp. Additionally, fingers need to apply requisite forces to hold the dish tight while it is transported to the dish rack. Compliance again becomes critical while placing the dish, allowing the dish to settle into one of the dish rack slots without being overconstrained by the fingers. Out of twenty test runs, sixteen were successful (80% success rate.) Visualization of this task is provided in Figure 5.

2) Napkin Pickup: Picking flat objects with no clearance from the surface necessitates compliance. In theory one can pick up the napkin by commanding a non-compliant gripper, but it would require sub-millimeter precision (a feat that is challenging for visual perception). Because our design is compliant, we purposefully drive the manipulator into the table which bends the fingers against the table, and then we close the fingers while moving up. Figure 5 shows it leads to the successful pickup of a napkin.

3) Strawberry Pickup: We chose this task to simultaneously demonstrate the speed and compliance of the fingers. We lowered the gain of the position controller in this case, which allowed us to grasp the strawberry gently along with our compliance and not damage the strawberry. We grasped the strawberry successfully over a dozen times without any visible damage on the strawberry

VI. Conclusion

In this work, we were able to obtain functional requirements for a useful robotic hand, we made an actuator that could obtain these specs, and then we built a two finger hand to validate the actuator's traits. Many other robotic hands try reach or exceed maximum human performance, and thus they are large and have unnecessary complexity. We've built a simpler hand design to do everyday tasks.

Our hand is wider in the knuckle portion, which means that it would be hard to fit 5 fingers in a future iteration, but a 3 and 4-finger hand is still possible. Future work involves making a 3-finger version that is fully dexterous, a wrist, and integrating tactile sensing. While our method for estimating the force and bandwidth requirements is a great step in understanding performance requirements, further work needs to be done to gather data from humans directly at the joint-level.

VII. Acknowledgements

The contributions for this paper are listed on our website. We thank the members of the Improbable AI Lab for helpful discussions and feedback. This research was supported by funding from Toyota Research Institute.

REFERENCES

[1] Wonik Robotics , Allegro Hand, 2023, http://wiki.wonikrobotics.com/AllegroHandWiki/index.php/Allegro_Hand, [Online; accessed Sep. 2023].

[2] Aadeel Akhtar. "3D-printing hands that feel". In: *GetMobile: Mobile Computing and Communications* 24.4 (2021), pp. 10–16.

[3] OpenAI: Marcin Andrychowicz et al. "Learning dexterous in-hand manipulation". In: *The International Journal of Robotics Research* 39.1 (2020), pp. 3–20.

[4] Ankit Bhatia, Aaron M Johnson, and Matthew T Mason. "Direct drive hands: Force-motion transparency in gripper design". In: *Robotics: science and systems*. 2019.

[5] Antonio Bicchi. "Hands for dexterous manipulation and robust grasping: A difficult road toward simplicity". In: *IEEE Transactions on robotics and automation* 16.6 (2000), pp. 652–662.

[6] L. B. Bridgwater et al. "The Robonaut 2 hand - designed to do work with tools". en. In: *2012 IEEE International Conference on Robotics and Automation*. St Paul, MN, USA: IEEE, 2012, 3425–3430.

[7] Lyndon B Bridgwater et al. "The robonaut 2 hand-designed to do work with tools". In: *2012 IEEE International Conference on Robotics and Automation*. IEEE. 2012, pp. 3425–3430.

[8] Ruben Castro Ornelas. "Robotic Finger Hardware and Controls Design for Dynamic Piano Playing". en. In: (2022). Accepted: 2022-08-29T16:03:48Z.

[9] Tao Chen et al. *Visual Dexterity: In-hand Dexterous Manipulation from Depth*. 2022. arXiv: 2211.11744 [cs.RO].

[10] Siegfried Derler and L-C Gerhardt. "Tribology of skin: review and analysis of experimental results for the friction coefficient of human skin". In: *Tribology Letters* 45 (2012), pp. 1–27.

[11] Peter Florence, Lucas Manuelli, and Russ Tedrake. *Self-Supervised Correspondence in Visuomotor Policy Learning*. 2019. arXiv: 1909.06933 [cs.RO].

[12] Erico Guizzo. *Building a Super Robust Robot Hand - IEEE Spectrum*. en.

[13] Ankur Handa et al. "DeXtreme: Transfer of Agile In-hand Manipulation from Simulation to Reality". In: *arXiv preprint arXiv:2210.13702* (2022).

[14] Yongqiang Huang and Yu Sun. "A dataset of daily interactive manipulation". In: *The International Journal of Robotics Research* 38.8 (2019), p. 8790886.

[15] Marco Hutter et al. "Anymal-a highly mobile and dynamic quadrupedal robot". In: *2016 IEEE/RSJ international conference on intelligent robots and systems (IROS)*. IEEE. 2016, pp. 38–44.

[16] S. Jacobsen et al. "Design of the Utah/M.I.T. Dextrous Hand". In: *1986 IEEE International Conference on Robotics and Automation Proceedings*. Vol. 3. 1986, 1520–1532.

[17] Benjamin Katz, Jared Di Carlo, and Sangbae Kim. "Mini cheetah: A platform for pushing the limits of dynamic quadruped control". In: *2019 international conference on robotics and automation (ICRA)*. IEEE. 2019, pp. 6295–6301.

[18] Gagan Khandate, Maximilian Haas-Heger, and Matei Ciocarlie. "On the feasibility of learning finger-gaiting in-hand manipulation with intrinsic sensing". In: *2022 International Conference on Robotics and Automation (ICRA)*. IEEE. 2022, pp. 2752–2758.

[19] C. Mittermayer and A. Steininger. "On the determination of dynamic errors for rise time measurement with an oscilloscope". In: *IEEE Transactions on Instrumentation and Measurement* 48.6 (1999), pp. 1103–1107.

[20] OpenAI et al. *Learning Dexterous In-Hand Manipulation*. 2019. arXiv: 1808.00177 [cs.LG].

[21] C Piazza et al. "A century of robotic hands". In: *Annual Review of Control, Robotics, and Autonomous Systems* 2 (2019), pp. 1–32.

[22] Andrew SaLoutos et al. "Towards Robust Autonomous Grasping with Reflexes Using High-Bandwidth Sensing and Actuation". In: arXiv:2209.11367 (2022). arXiv:2209.11367 [cs].

[23] *Shadow Dextereous Hand*. Shadow Robot, Shadow Hand, https://www.shadowrobot.com/dexterous-hand-series/, [Online; accessed Sep. 2023].

[24] Kenneth Shaw, Ananye Agarwal, and Deepak Pathak. *LEAP Hand: Low-Cost, Efficient, and Anthropomorphic Hand for Robot Learning*. 2023. arXiv: 2309.06440 [cs.RO].

[25] Jun Shintake et al. "Soft robotic grippers". In: *Advanced materials* 30.29 (2018), p. 1707035.

[26] Alexander Slocum. *FUNdaMENTALS of Design*. FUNdaMENTALS of Design , 7- Power Systems, http://pergatory.mit.edu/resources/fundamentals.html, [Online; accessed Sep. 2023].

[27] Bai-Yang Sun et al. "A science-driven method for determining morphological parameters of prosthetic hands". In: *Bioinspiration and Biomimetics* 16.4 (2021), p. 046017.

[28] Patrick M Wensing et al. "Proprioceptive actuator design in the mit cheetah: Impact mitigation and high-bandwidth physical interaction for dynamic legged robots". In: *Ieee transactions on robotics* 33.3 (2017), pp. 509–522.

[29] Wenxuan Zhou and David Held. *Learning to Grasp the Ungraspable with Emergent Extrinsic Dexterity*. 2022. arXiv: 2211.01500 [cs.RO].

[30] Henry Zhu et al. "Dexterous manipulation with deep reinforcement learning: Efficient, general, and low-cost". In: *2019 International Conference on Robotics and Automation (ICRA)*. IEEE. 2019, pp. 3651–3657.